Physiological and molecular characterization of the late ripening stages in Mangifera indica cv Keitt

--Manuscript Draft--

Manuscript Number:	
Article Type:	Research Paper
Keywords:	Mangifera indica, post-climacteric ripening, commercial shelf life, softening, ethylene, DA-meter, qRT-pcr.
Corresponding Author:	Nicola Busatto Fondazione Edmund Mach Centro Ricerca e Innovazione ITALY
First Author:	Nicola Busatto
Order of Authors:	Nicola Busatto
	Lorenzo Vittani
	Brian Farneti, PhD
	Iuliia Khomenko
	Matteo Caffini
	Simone Faccini
	Marco Boschetti
	Fabrizio Costa
Abstract:	Mango is heavily affected by rapid off-tree ripening progression with an excessive fruit softening that eventually limits its marketability. The comprehension of the physiological events occurring in the post-climacteric/senescent phase can contribute to the identification of possible solutions for the improvement of shelf life. In this scenario, the ripening process of mangoes cv Keitt was monitored for two weeks in a simulated commercial shelf life, after shipping from Brazil to Italy, measuring both ripening-associated parameters (firmness, soluble solid content, ethylene production) and non-destructive method based on Vis/NIR spectroscopy (the ripening index I_{AD}). Moreover, the expression pattern of thirteen genes related to different ripening aspects such as ethylene biosynthesis (ACS , ACO), perception (ETR , ERS) and signaling (EIN2 , ERF), in combination with genes responsible for cell wall metabolism (PG14 , PG21 , EXP , PEL , CEL) and carotenoids accumulation (PSY , NCED) were assessed. The results highlighted a specific gene signature characterizing the post-climacteric softening and the senescence onset. Moreover, the non-destructive I_{AD} has proven to be an effective non-destructive monitoring system of the fruit ripening in mango.
Suggested Reviewers:	

	expert in genetics and plant breeding
	Geroge Manganaris, PhD Prof, Cyprus University of Technology: Technologiko Panepistemio Kyprou george.manganaris@cut.ac.cy expert in fruit physiology and postharvest
Opposed Reviewers:	

Dear Prof. Chris Watkins, Editor in Chief of Postharvest Biology and Technology.

Enclosed to this cover letter I am sending to your attention the following manuscript entitled: "Physiological and molecular characterization of the late ripening stages in *Mangifera indica* cv Keitt".

Mango is one of the most cultivated tropical fruit world-wide, but it is characterized by a short shelf-life due to its high perishable nature, which strongly limits its marketability. Mango, as well as many other tropical fruits, is susceptible to chilling injuries making it not suitable for cold storage. Moreover, the most common strategies used to extend its shelf life are controlled atmosphere or film coating, two effective but expensive approaches that require specialized facilities. On the other hand, the application of 1-MCP to this deliquescent drupe can result in an excessive firmness retention and a low aromatic profile, resulting in a detrimental impact on the consumer's appreciation.

Therefore, the understanding of the physiological events related in particular to pulp over-softening and senescence onset could greatly facilitate the post-harvest management of mango.

For this reason, fruit cultivar Keitt were shipped from Brazil to Italy and underwent to a prolonged shelf life (two weeks) in order to monitor the post-harvest ripening progression in a commercial scenario. The fruit ripening was assessed through the analysis of important standard parameters, such as firmness, soluble solid content, ethylene production, together with a non-destructive and sophisticated methodology based on Vis/NIR spectroscopy (the ripening index I_{AD}). These data were moreover correlated with the expression profile of thirteen genes involved in the biosynthesis (*ACS*, *ACO*), perception (*ETR*, *ERS*) and signaling (*EIN2*, *ERF*) of the hormone ethylene, in addition to elements responsible for cell wall metabolism (*PG14*, *PG21*, *EXP*, *PEL*, *CEL*) and carotenoids accumulation (*PSY*, *NCED*).

Our findings highlighted the existence of a specific regulation in the network of enzymes acting in the softening process during the ripening of Keitt mango. In fact, while the initial drop of firmness can be correlated to the expression of *PEL* and *CEL*, the initiation of the senescence can be associated to *PG14*, *PG21* and *EXP*. This comprehensive investigation allowed a more precise and informative characterization of the postharvest ripening of fruit of mango harvested at horticultural maturity and shipped overseas. The expression profile we showed could represent a new molecular diagnostic tool for further investigation about the quality features of mango internationally commercialized.

I hope this manuscript could meet your expectation and be considered for publication in your highly estimated journal, and please, do not hesitate to contact me for any additional info.

Best wishes

Nicola Busatto

Highlights

- specific molecular regulation characterizes Mango post-climacteric ripening
- senescence phase is coordinated by the expression of ACS and ACO
- differential activation of cell wall-related genes determines the pulp softening
- dramatic loss of firmness is the major change during Mango post-harvest ripening

1   **Physiological and molecular characterization of the late ripening stages in _Mangifera_**

2   **_indica_ cv Keitt.**

3

4   Nicola Busatto[1], Lorenzo Vittani[2], Brian Farneti[1], Iuliia Khomenko[3], Matteo Caffini[4],Simone

5   Faccini[4], Marco Boschetti[4], Fabrizio Costa[1,2].

6

7   [1] Department of Genomics and Biology of Fruit Crops, Research and Innovation Centre,

8   Fondazione Edmund Mach, via Mach 1, 38010 San Michele all'Adige, Trento, Italy

9   [2] Center Agriculture Food Environment C3A, University of Trento, Via Mach 1, 38010 San

10   Michele all'Adige (Trento), Italy

11   [3] Department of Food Quality and Nutrition, Research and Innovation Centre, Fondazione

12   Edmund Mach, via Mach 1, 38010 San Michele all'Adige, Trento, Italy

13   [4]Microtec, Via Julius-Durst Straße 98 39042 Bressanone / Brixen Italy

14

15

16   Corresponding author: nicola.busatto@fmach.it

17

18

19

20

21

22

23

24

25

26 ABSTRACT

27 Mango is heavily affected by rapid off-tree ripening progression with an excessive fruit

28 softening that eventually limits its marketability. The comprehension of the physiological

29 events occurring in the post-climacteric/senescent phase can contribute to the identification of

30 possible solutions for the improvement of shelf life. In this scenario, the ripening process of

31 mangoes cv Keitt was monitored for two weeks in a simulated commercial shelf life, after

32 shipping from Brazil to Italy, measuring both ripening-associated parameters (firmness, soluble

33 solid content, ethylene production) and non-destructive method based on Vis/NIR

34 spectroscopy (the ripening index I_{AD}). Moreover, the expression pattern of thirteen genes

35 related to different ripening aspects such as ethylene biosynthesis (*ACS*, *ACO*), perception

36 (*ETR*, *ERS*) and signaling (*EIN2*, *ERF*), in combination with genes responsible for cell wall

37 metabolism (*PG14*, *PG21*, *EXP*, *PEL*, *CEL*) and carotenoids accumulation (*PSY*, *NCED*) were

38 assessed. The results highlighted a specific gene signature characterizing the post-climacteric

39 softening and the senescence onset. Moreover, the non-destructive I_{AD} has proven to be an

40 effective non-destructive monitoring system of the fruit ripening in mango.

41

42

43 <u>Keywords</u>

44 *Mangifera indica*, post-climacteric ripening, commercial shelf life, softening, ethylene, DA-

45 meter, qRT-pcr.

46

47

48

49

50

INTRODUCTION

Mango (*Mangifera indica* Linn.), belonging to the *Anacardiaceae* family, is the second most important fruit crop widely cultivated in tropical and subtropical countries, characterized by a climacteric ripening behavior, in which a peak in the respiration rate is concomitant with an outburst of ethylene production (Singh et al., 2013). In climacteric fruit ethylene, besides promoting stress response and senescence processes (Alós et al., 2018), oversees and regulates most of the events associated to the ripening syndrome (Gapper et al., 2013; Osorio et al., 2013). The ethylene synthesis pathway branches from the Young cycle and comprises two committed steps: ACC synthase (*ACS*) converting S-adhenosyl-methionine into 1-aminocyclopropane-1-carboxylic acid (ACC), which in turn is finally oxidized to ethylene by the action of ACC oxidize (*ACO*) (Van Der Straeten et al., 2020). This gaseous phytohormone is further perceived by a family of ethylene receptors (*ETR*s) (Binder, 2008), characterized by specific histidine-kinase activity, localized in the endoplasmatic reticulum that triggers the downstream signal perception and allows the stabilization of the ethylene response factor (*ERF*). ERF transcription factors, binding the promoter regions of ethylene responsive genes, can induce the activation of ripening related modification, such as texture modifications, color changes, production of volatiles and aroma, and degradation of starch into soluble sugars (Seymour et al., 2013).

In mango, the rapid ripening kinetics can limit the shelf life to few weeks after harvest (Paul et al., 2019; Schouten et al 2018). Similarly to other tropical fruits, mango is also highly susceptible to chilling injuries making it not suitable for cold storage at temperatures below 13 °C (Singh et al., 2013), severely compromising the marketability of this fruit. The limited storability and the typical over-ripening process of this fruit species are the major cause of the low quality perceived by consumers. To delay over-ripening, a possible solution can be offered by the exogenous application of 1-methyl-cyclo-propene (1-MCP), a synthetic cyclic olephin

76 binding ethylene receptors and consequently avoiding the downstream signal transduction,

77 impairing the ethylene dependent pathway responsible for the fruit ripening in climacteric

78 species (Watkins, 2006; Zhang et al., 2020). However, the suppression of the ethylene

79 perception leads to a severe downregulation of the pathways responsible for the development

80 of volatile molecules (El Hadi et al., 2013) that in mango are an essential constituents of the

81 complex fruit aroma and quality such as: monoterpenes, esters and aldehydes (Lalel et al.,

82 2003). Moreover, mango is classified as a deliquescent drupe, therefore the effect of 1-MCP

83 can result in an excessive retention of firmness, with a negative impact on the perception of

84 fruit quality, similarly to what has been observed in pear (Chiriboga et al., 2011).

85 Other alternative strategies to improve shelf life performance are represented by controlled

86 atmosphere or film coating (Dang et al., 2008), two effective but expensive strategies requiring

87 specialized storage facilities. Therefore, the mango supply chain is still suffering from

88 limitations determined by the lack of effective and inexpensive methodologies allowing an easy

89 and sustainable maintenance of fruit quality over the commercialization process. Moreover, the

90 employment of reliable and non-destructive methodologies addressed to the monitoring of the

91 ripening progression, could greatly facilitate the post-harvest management, as for apple and

92 peach (Farneti et al., 2015; Kasim et al. 2021).

93 Fruit quality can also be improved through a better understanding and comprehension of the

94 ripening processes. To this end, a whole transcriptomic analysis based on RNA-seq has been

95 carried out to describe the ripening process in mango (Dautt-Castro et al., 2015; Srivastava et

96 al., 2019), discriminating the different members of the polygalacturonases multigene family

97 responsible of the flesh softening (Dautt-Castro et al., 2019), with particular regards to the

98 transition from unripe to ripe stage. However, the characterization of the late ripening stage is

99 still lacking.

100 In this work we assessed the kinetics of important agronomical parameters, such as vis-nir DA

101 ripening index (I_{AD}), soluble solid content (SSC), texture modifications (F_1) and ethylene

102 production ($\mu L\ Kg^{-1}$) during the late ripening stage of mango fruit cv Keitt in a commercial

103 simulation. These data were correlated with the expression profile of a set of candidate genes

104 belonging to different biochemical pathways well known to be involved in the ethylene

105 pathway (both synthesis and perception) and other important quality traits.

106

107 MATERIALS AND METHODS

108

109 <u>Plant material</u>

110 Mango fruit *cv* Keitt were harvested in a commercial orchard in Brazil and promptly shipped

111 to Italy in a refrigerated container (2 weeks at 8 °C), following the standard commercial

112 procedure. After the delivery to the laboratory (1d), the fruit were maintained in a shelf life

113 condition at 20 °C (room temperature) for two weeks and sampled every four days for four

114 times and named accordingly: 5d, 9d, 12d, 15d.

115

116 <u>Non-Destructive Analysis</u>

117 Four trays containing 9 fruit each were periodically photographed and used for assessing the

118 shelf life ripening progression at each timepoint using a DA-Meter, a portable non-destructive

119 device based on a visible/Near Infra Red (Vis/NIR) spectroscopy (TR, Forli, Italy). This device

120 enables the measurement of the DA Index (I_{AD}), a parameter related to the amount of

121 chlorophyll and ranging from 2,2 to 0, for less and fully ripe stage of the fruit, respectively

122 (Ziosi et al., 2008). The I_{AD} measurements were also made on a second batch of 5 fruit/time

123 point, sampled for the destructive and molecular analysis. The I_{AD} values were reported as

124 average of three independent measurements/fruit.

125

126 <u>Destructive Analysis</u>

127 The assessment of fruit texture was carried out with a computer-controlled texture analyzer

128 TA-XTplus (StableMicroSystem, Godalming, UK) The mechanical displacement profile was

129 obtained from four peeled portion of flesh around the equatorial region of each fruit. The

130 texture analyzer operated through a compression mode according to the following instrument's

131 setting: test speed of 300 mm/min, target mode at a distance of 15 mm with a trigger force

132 threshold of 5 g. The mechanical displacement was acquired with a 5 kg loading cell with a

133 resolution of 500 points per second.

134 The mango juice of each fruit (3 replicates per each fruit) was employed for measuring the total

135 soluble solids (SSC; %) with a digital hand-held refractometer (Atago, Tokyo, Japan).

136

137 <u>Ethylene quantification</u>

138 Ethylene, from 3 replicates each one resulting from five pooled fruit, was measured with a

139 PTR-ToF-MS 8000 apparatus (Ionicon Analytik GmbH, Innsbruck, Austria) equipped with

140 switchable reagent ion system that allowed the operation of the instrument in H_3O^+ and O_2^+

141 modes, as described by Cappellin et al.(2014). 0.5 g of powdered frozen tissue was rapidly

142 inserted into a 20 mL glass vial equipped with PTFE/silicone septa (Agilent, Santa Clara, CA,

143 USA) and mixed with 0.5 mL antioxidant solution, and preserved at 4 °C until assessment.

144 Count losses due to the ion detector dead time were corrected off-line through a Poisson

145 statistics-based method while internal calibration was performed according to the procedure

146 described in Cappellin et al. (2011a, 2011b). A custom built calibration system based on flow

147 controllers (MKS, Andover, MA) was used to dilute ethylene standard (1 ppmv) with zero air

148 (generated by a Gas Calibration Unit, Ionicon Analytik GmbH). Measurements were done with

149 the PTR-ToF-MS in O_2^+mode (Cappellin et al., 2014).

150

151 <u>Gene expression analysis by RT-qPCR</u>

152 From pulp tissues of the mangoes used for the destructive analysis (five pooled fruit for each

153 timepoint), total RNA was extracted with the Spectrum Plant total RNA kit (Sigma-Aldrich)

154 and further controlled for quantity and quality with a NanoDrop ND-8000 (ThermoFisher

155 Scientific, MA, USA) and a 2100 Bioanalyzer (Agilent Technologies, CA, USA), respectively.

156 2 μg of extracted RNA were further treated with 2 units of Ambion DNAse and further

157 converted into cDNA with the "SuperScript" VILO cDNA Synthesis kit (ThermoFisher

158 Scientific, MA, USA). The expression of thirteen genes (Suppl. Tab.1) was carried out with

159 the ViiA7 using the FAST SYBR GREEN MASTER MIX (Thermofisher Scientific, MA,

160 USA). The Real Time qPCR reaction was performed with the following thermal profile: 95 °C

161 20 s, 40 cycles of 95 °C 1 s and 60 °C 20 s and finishing with a final cycle at 95 °C 15 s, 60 °C

162 60 s and 95 °C per 15 s, to define the reaction melting curve. The gene expression was reported

163 by the mean normalized expression through the use of the equation 2 of the "Qgene" software

164 according the indication described in Simon (2003).

165 The primer pairs employed for the gene expression profiling were retrieved from literature,

166 based on their compatibility with the FAST protocol. The gene actin (*ACT*) was used as

167 housekeeping.

168

169 <u>Data analysis</u>

170 The data were analyzed with R using the ChemometricswithR package (Wehrens, 2011) and

171 Excel.

172 The force mechanical displacement of each texture measurement was digitally analyzed and

173 processed with the software Exponent v4 (Stable MicroSystem). Through a dedicated macro,

174 6 parameters were defined to characterize the mechanical properties of each fruit collected at

175   each stage, such as the yield point (transition point from the elastic to the plastic phase), the

176   gradient (or elasticity module), the area defined by the mechanical displacement curve and

177   three force values identified over the profile (minimum, maximum and mean force value).

178   Tukey HSD test ($\alpha = 0.05$) has been performed using the software R in order to indicate

179   significative differences between the different sampling time.

180

181   RESULTS

182   <u>1. Fruit quality assessment during the shelf life ripening in mango</u>

183   During the two weeks of shelf life, three parameters associated to the ripening progression were

184   assessed: I_{AD}, soluble solid content (SSC), and firmness. As showed in Fig.1a, the I_{AD} values

185   progressively decrease over the five timepoints included in the experimental design from 2.1

186   at 1d to 1.37 at 15d. As expected, the standard deviation calculated on five fruit, increased

187   during the monitoring time, spanning from 0.08 to 0.38 corresponding to 3.7 % and 27.8 % of

188   the average I_{AD} value at 1d and 15d, respectively, indicating that ripening progressed following

189   a heterogeneous pattern, magnifying the physiological differences existing at the harvest time

190   among the fruit. The I_{AD} declined starting from 5d stage, showing a constant reduction until

191   15d, where a more distinct drop was observed (Fig.1a). A similar pattern was also observed in

192   the mangos contained in the other batches, continuously monitored during the two weeks of

193   the survey, validating the profile of the I_{AD} we observed on the first batch (Suppl. Fig.1a and

194   Suppl. Fig.2). Moreover, a set of fruit was also photographed at each timepoint allowing the

195   visual inspection of the ongoing off-tree ripening process (Suppl. Fig.1b).

196   The analysis of fruit texture carried out with a texture analyzer evidences a rapid texture decay

197   between the 1d and 5d stages, declining from its maximum average level of 50.7 N to 5.6 N,

198   respectively. It is worth noting that, from 9d to 15d the loss of firmness proceeded less

199   intensively, reaching at 15d a value of 1.25 N, corresponding to a complete cell wall

200   degradation, resulting in a deliquescent flesh (Fig.1b).

201   This aspect can also be highlighted by the modification of the mechanical profile measured by

202   the TA-XTplus (Fig. 2) and obtained as response to compressions exerted by the probe. In fact

203   the compression slope observed until the yield point (F1), that marks the transition from the

204   elastic (reversible) to the plastic phase of the material (irreversible crushing) progressively

205   faded, being totally undetectable starting from the timepoint 9d.

206   Conversely, the soluble solid content (SSC) did not show any consistent change over the time

207   course (Fig.1c), with a maximum level of 13.5 at 5d and a minimum of 10.4 at 1d. The other

208   timepoints showed instead an SSC values spanning from 11.8 to 12.7.

209   The ethylene level was highly accumulated at the initial stage of the time course, with the

210   highest value of 417 μL Kg^{-1} assessed at 9d stage, after which it declined progressively towards

211   the 15d stage (Fig. 1d). The value of ethylene of 247 μL Kg^{-1} assessed at 1d indicated that the

212   fruit of mango were already in the climacteric phase at the beginning of the shelf life

213   postharvest time course.

214

215   2. Expression analyses of genes belonging to the ethylene domain.

216   The ripening behavior of the fruit of mango in shelf life ripening was also transcriptionally

217   investigated through the analysis of the expression pattern of 6 specific genes. The first two

218   genes, *ACS* (1-aminocyclopropane-1-carboxylic acid synthase) and *ACO* (1-

219   aminocyclopropane-1-carboxylic acid oxidase), are responsible for the synthesis of this

220   phytohormone, while *ETR1* (ethylene receptor 1), *ERS1* (ethylene response sensor 1) and *EIN2*

221   (ethylene insensitive 2) are involved in the perception and signal transduction of the ethylene

222   signal. The final step of the ethylene pathway is represented by ERF (ethylene response factor),

223   a typical member of a multigene family of transcription factors that contribute to modulate the

224 expression of the genes responsible for the modifications taking place during the ripening

225 syndrome (Chen et al., 2005). Among this set of genes, the two elements involved in ethylene

226 production, *ACS* and *ACO*, showed a transcriptional accumulation during the monitoring shelf

227 life postharvest ripening, from 1d to 15d (Fig.3a and b), with the highest value observed in 15d

228 stage. The expression of the elements involved in the signaling and signal-transduction

229 pathway (*ETR1*, *ERS1* and *ERF*) were instead more expressed at the initial stage of the time

230 course (Fig.3c, d and f), while the *EIN2* gene (Fig.3e) showed a more linear and constitutive

231 type of expression.

232

233 3. Modulation of the genes involved in ripening-related processes.

234 The post-climacteric ripening phase was further investigated analyzing the expression of genes

235 involved in the dismantling of the cell wall and middle lamella polysaccharide architecture and

236 synthesis of carotenoids. For the control of fruit texture, we selected two members of the *PG*

237 (polygalacturonase) family, *PG14* and *PG21*, together with three genes involved in the primary

238 cell wall physiology, namely *EXP* (expansine), *PEL* (pectate lyase) and *CEL* (cellulase) (Dautt-

239 Castro et al., 2019; Tucker et al., 2017). The analysis of the transcript profile showed two

240 distinct patterns. While the expression of *PG14*, *PG21* and *EXP* (Fig.4a, b, c) increased over

241 the time course, reaching the maximum level at 15d, the transcript accumulation of *PEL* (Fig.

242 4d) and *CEL* (Fig.4e) displayed a progressive decrease over the time course, both reaching their

243 minimum level at 15d.

244 In addition to the metabolism of the cell wall metabolism, the accumulation of carotenoids is

245 another important quality attribute for mango. In this regards we investigated the expression

246 profile of two important genes involved in this pathway, *PSY* and *NCED*. *PSY* (a phytoene

247 synthase) was highly expressed until the 9d stage, after which decreased through 12d and 15d

248 stages (Fig. 4f). The 9d stage was also interested by the highest expression value of *NCED* (9-

249   cis-epoxycarotenoid dioxygenase), which, similarly to *PSY*, decreased towards the end of the

250   time course (15d stage; Fig. 4g).

251

252   4. Multivariate analysis allows a characterization of the off-tree fruit ripening.

253   A multivariate analysis was used to visualize the distribution of the samples considering the

254   variability captured by the different entities we assessed in this work to characterize the late

255   ripening phase of mango. The 2D-PCA plot (Fig.5a), accounting for 84.4 % of the total

256   variance, clearly distinguished the different samples on the PCA space separating the five

257   timepoints in three distinct groups. 1d and 5d stages, corresponding to the initial phases of the

258   shelf life ripening, were grouped in the quadrant I, characterized by negative values of PC1 and

259   positive values of PC2. The two following samples, 9d and 12d stages, were described by

260   negative values of PC2 and located in the quadrants II and III, respectively. 15d stage, the last

261   timepoint comprised in the survey, was instead positioned in the quadrant IV, identified by

262   positive values of both PC1 and PC2. It is worth noting, that the position of the first group (1d,

263   5d) was strongly influenced by the projections of the vectors assigned to high firmness values

264   and the expression profile of genes encoding for both, ethylene receptors (Fig.5b) and cell wall-

265   related enzymes (*CEL* and *PEL*). The second group, comprising 9d and 12d stages, was mainly

266   characterized by the loading vectors depicting soluble solid accumulation, carotenoids

267   catabolism and ethylene quantification. In the end, the 15d stage was characterized by the

268   vector projections corresponding to the genes responsible for the ethylene synthesis (*ACS* and

269   *ACO*) and by two genes involved in the cell wall disassembly (*PG14* and *EXP*).

270

271   DISCUSSION

272   1. A bi-modal gene activation is involved in the textural changes of the late ripening phase in

273   mango.

274 The major phenotypical change observed during this commercial simulation was represented

275 by an excessive softening, which is the main factor limiting mango shelf life, storage, and

276 marketability. The highest rate of change for this parameter was observed at the beginning of

277 the time course, between 1d and 5d stages that exhibited a decrease from 50.1 N, to 5.6 N,

278 value below the threshold usually considered for consumer appreciation ($\simeq$ 15.6 N) (Nassur et

279 al., 2015). Full ripe fruit of mango are normally characterized by firmness values of about 4-5

280 N, assessed in our experimental design at 5d stage. The lower firmness levels we observed in

281 the range 9d-15d stages, demonstrated the ongoing of the off-tree ripening progression and the

282 shift from an over-ripe condition to a final senescence. Observing the expression pattern of the

283 cell-wall related genes included in this study, it is possible to note a differential timing of

284 activation of *PEL* and *CEL*, respect to *PG14*, *PG21* and *EXP*. While the first group exhibited

285 the highest expression level during the first two timepoints (1d and 5d), in concomitance with

286 the most evident loss of firmness ($\rho = 0.78$ and 0.70, respectively), the expression level of the

287 second group of genes, even if already expressed in the first stages, constantly increased

288 towards the 15d stage, characterized by the lowest firmness value ($\rho = -0.60$, -0.42 and -0.35

289 respectively). This result might suggest a particular involvement of *PEL* and *CEL* during the

290 initial phase of cell wall breakdown, while *PG14, PG21* and *EXP* exhibited an activity more

291 associated to the senescence onset in mango. *CEL* is a member of the endo-β-1,4-glucanase

292 multigene family that has been already isolated and studied in mango, cv Dashehari (Chourasia

293 et al., 2008; Srivastava et al., 2019). The role of this gene in decreasing the content of cellulose

294 and hemicellulose was associated to the initiation and the control of the initial stages of fruit

295 ripening. Chourasia and colleagues also suggested that the pectin degradation in mango could

296 be primarily regulated by the action of pectate lyase hydrolase, consistent with the expression

297 profile of the *PEL* gene observed in this work. In addition, we monitored the expression level

298 of other two pectolytic enzymes encoding genes, *PG21* and *PG14,* recently isolated in mango

299   (Dautt-Castro et al., 2019). PG21 is particularly expressed throughout the whole ripening

300   progression, while the transcript of *PG14* is more accumulated in the senescent stage (Dautt-

301   Castro et al., 2019). Hence, the high expression level of *PG14* at 9d, 12d and 15d stages can be

302   used as markers to define the physiological transition between over-softening and senescence.

303   Interestingly, both *PG21* and *PG14* enzymes are characterized by endo-PG activity, and in

304   peach, a drupe with rheological characteristic similar to mango, it has been demonstrated that

305   endo-PGs accumulate only in melting varieties, coincident with the melting phase (Brummell

306   et al., 2004). In the end, the similar expression profile of *EXP* with regards to the two *PG*s

307   tested, suggested a synergic enzymatic activity addressed to the loosening of the cell wall

308   structure by increasing the relative movement among polymers, as already observed in different

309   fruits (Brummell and Harpster, 2001; Dautt-Castro et al., 2015).

310

311   2. The late ripening phase in mango is coordinated by the expression of *ACS* and *ACO* genes.

312   The post-harvest ripening of mango mostly relays on the hormone ethylene. During the shelf

313   life at room temperature, *ACS* and *ACO*, the two key genes for the ethylene biosynthesis,

314   showed a progressive increase during the time course, with the maximum expression shown at

315   the last timepoint. Interestingly, the expression level of *ACO* anticipated the transcript of *ACS*,

316   without showing any significant variation from 1d to 12d. This aspect represents a typical

317   transcriptional signature of the mango fruit ripening, already observed in other works showing

318   that these two genes were transcriptionally undetectable in unripe fruits while increasing

319   considerably in full ripening stage, with the expression of *ACO* preceding the transcript of *ACS*

320   (Cruz-Hernández and Gómez-Lim, 1995; Singh et al., 2013). A possible explanation of this

321   phenomenon could be represented by the different mechanisms of regulation existing in these

322   two genes. While the expression of *ACO* is normally modulated at transcriptional level, the

323   activity of *ACS* is instead mainly controlled by post-transcriptional regulation (Pattyn et al.,

324 2021), through specific phosphorylation targeting C-terminal conserved moieties on type-1 and

325 type-2 ACS protein (Kamiyoshihara et al., 2010). It is also worth noting that the ethylene

326 quantification pattern is not completely consistent with the expression profile of *ACS* and *ACO*,

327 in particular at 12d and 15d stages. This aspect is a possible consequence of the ongoing

328 senescence processes that characterize 12d and 15d timepoints. A similar trend was observed

329 also in tomato (Van de Poel et al., 2012) during post-climacteric ripening, where, despite the

330 remarkable decrease of ethylene production physiologically occurring after the climacteric

331 peak and at the beginning of the senescence stages, an upturn in the expression levels of

332 Le*ACO1* and especially *LeACS4* was detected, without a coherent recovery of the ethylene

333 production. In late ripening/senescent stage in tomato fruit it was moreover shown that, in

334 agreement to what we observed in mango in this work, the other elements involved in ethylene

335 perception and signaling (such as *ETR1, ERS1, EIN2* and *ERF*) were down regulated, with an

336 opposite trend respect the ethylene biosynthetic genes (Liu and Franks, 2015).

337

338 3. Transcriptional signature of the late fruit ripening/senescent phase in mango.

339 The Principal Component Analysis plot computed through the employment of different types

340 of traits (gene expression and fruit ripening phenotypic assessment) clearly distinguished fruit

341 in late ripening (1d-9d) and in senescent phase (12d-15d). After 5d stage, fruit of mango

342 initiated a progressive over-ripening process leading to a deliquescent aspect of the fruit flesh,

343 which contributed to a higher susceptibility and vulnerability to the development of disease

344 typical of the fruit senescence phase. The senescent phase (12d and 15d stages), resulted to be

345 genetically controlled by the ethylene-dependent expression of *PG14, PG21* and *EXP*, involved

346 in important dismantling process of the polysaccharidic structure of the cell wall and middle

347 lamella complex (Brummell et al., 2004; Dautt-Castro et al., 2019; Payasi et al., 2009;

348 Srivastava et al., 2019; Uluisik and Seymour, 2020). It is worth noting, that the samples at 12d

349 are located on the third quadrant of the PCA space (Fig.4a) defined by the vectors representing

350 the total soluble solid content (SSC) and the expression of *NCED* (Fig.4b), the main rate

351 limiting step of the abscisic acid (ABA) synthesis (Chen et al., 2020; Zhang, 2014). The ABA

352 fluctuations, following the carotenoids biosynthesis, are often associated with ripening,

353 senescence and ethylene production (Cherian et al., 2014; Zaharah et al., 2012). The expression

354 of *NCED* was in fact consistent with the ethylene production supporting the possible role of

355 ABA in regulating the fruit ripening process also in mango, as already hypothesized by Iqbal

356 et al. (2017). ABA is a hormone known to regulate the fruit ripening process in non-climacteric

357 fruits. In strawberry, the fruit ripening seems to be triggered by the synthesis of ABA and

358 coordinated by the accumulation of sugars (Luo et al., 2020). A similar controlling mechanism

359 could also play a role in the regulation of the late ripening in mango, but additional works are

360 needed to validate this hypothesis.

361

362 CONCLUSION

363 Mango is one of the main tropical fruit shipped and marked in distant countries, therefore, the

364 investigation of the ripening processes is essential prerequisite to guaranteed high quality fruit.

365 Among the aspects contributing to the appreciation of this fruit, the decay of fruit softening is

366 a crucial factor, considering the deliquescent type of texture of mango. An excessive softening,

367 typical of over-ripen/senescent stage is however one of the most important phenomena leading

368 to important fruit decay. The results presented in this work can be now considered as a new

369 tool suitable to better investigate the progression of fruit ripening for a more sophisticated and

370 informative postharvest management. The molecular profile of this gene set could depict the

371 progression of the entire process of fruit ripening and postharvest ripening, enabling the

372 identification of the crucial transition phase leading to fruit senescence and thus limiting its

373 marketability.

374

378

379   BIBLIOGRAPHY

380   Alós, E., Rodrigo, M.J., Zacarias, L., 2018. Ripening and senescence, Postharvest Physiology

381   and Biochemistry of Fruits and Vegetables. Elsevier Inc. https://doi.org/10.1016/B978-

382   0-12-813278-4.00007-5

383   Binder, B.M., 2008. The ethylene receptors: Complex perception for a simple gas. Plant Sci.

384   175, 8–17. https://doi.org/10.1016/j.plantsci.2007.12.001

385   Brummell, D.A., Dal Cin, V., Crisosto, C.H., Labavitch, J.M., 2004. Cell wall metabolism

386   during maturation, ripening and senescence of peach fruit. J. Exp. Bot. 55, 2029–2039.

387   https://doi.org/10.1093/jxb/erh227

388   Brummell, D.A., Harpster, M.H., 2001. Cell wall metabolism in fruit softening and quality

389   and its manipulation in transgenic plants. Plant Mol. Biol.

390   https://doi.org/10.1023/A:1010656104304

391   Cappellin, L., Biasioli, F., Granitto, P.M., Schuhfried, E., Soukoulis, C., Costa, F., Märk,

392   T.D., Gasperi, F., 2011a. On data analysis in PTR-TOF-MS: From raw spectra to data

393   mining. Sensors Actuators, B Chem. 155, 183–190.

394   https://doi.org/10.1016/j.snb.2010.11.044

395   Cappellin, L., Biasioli, F., Schuhfried, E., Soukoulis, C., Mark, T.D., Gasperi, F., 2011b.

396   Extending the dynamic range of proton transfer reaction time-of-flight mass

397   spectrometers by a novel dead time correction. Rapid Commun. Mass Spectrom. 25,

398   179–183. https://doi.org/10.1002/rcm.4819

399 Cappellin, L., Makhoul, S., Schuhfried, E., Romano, A., Sanchez Del Pulgar, J., Aprea, E.,

400   Farneti, B., Costa, F., Gasperi, F., Biasioli, F., 2014. Ethylene: Absolute real-time high-

401   sensitivity detection with PTR/SRI-MS. The example of fruits, leaves and bacteria. Int.

402   J. Mass Spectrom. 365–366, 33–41. https://doi.org/10.1016/J.IJMS.2013.12.004

403 Chen, K., Li, G.J., Bressan, R.A., Song, C.P., Zhu, J.K., Zhao, Y., 2020. Abscisic acid

404   dynamics, signaling, and functions in plants. J. Integr. Plant Biol. 62, 25–54.

405   https://doi.org/10.1111/jipb.12899

406 Chen, Y.F., Etheridge, N., Schaller, G.E., 2005. Ethylene signal transduction. Ann. Bot. 95,

407   901–915. https://doi.org/10.1093/aob/mci100

408 Cherian, S., Figueroa, C.R., Nair, H., 2014. "Movers and shakers" in the regulation of fruit

409   ripening: A cross-dissection of climacteric versus non-climacteric fruit. J. Exp. Bot. 65,

410   4705–4722. https://doi.org/10.1093/jxb/eru280

411 Chiriboga, M.A., Schotsmans, W.C., Larrigaudière, C., Dupille, E., Recasens, I., 2011. How

412   to prevent ripening blockage in 1-MCP-treated "Conference" pears. J. Sci. Food Agric.

413   91, 1781–1788. https://doi.org/10.1002/jsfa.4382

414 Chourasia, A., Sane, V.A., Nath, P., 2006. Differential expression of pectate lyase during

415   ethylene-induced postharvest softening of mango (Mangifera indica var. Dashehari).

416   Physiol. Plant. 128, 546–555. https://doi.org/10.1111/j.1399-3054.2006.00752.x

417 Chourasia, A., Sane, V.A., Singh, R.K., Nath, P., 2008. Isolation and characterization of the

418   MiCel1 gene from mango: Ripening related expression and enhanced endoglucanase

419   activity during softening. Plant Growth Regul. 56, 117–127.

420   https://doi.org/10.1007/s10725-008-9292-5

421 Cruz-Hernández, A., Gómez-Lim, M.A., 1995. Alternative oxidase from mango (Mangifera

422   indica, L.) is differentially regulated during fruit ripening. Planta 197, 569–576.

423   https://doi.org/10.1007/BF00191562

424   Dang, K.T.H., Singh, Z., Swinny, E.E., 2008. Edible coatings influence fruit ripening,

425   quality, and aroma biosynthesis in mango fruit. J. Agric. Food Chem. 56, 1361–1370.

426   https://doi.org/10.1021/jf072208a

427   Dautt-Castro, M., López-Virgen, A.G., Ochoa-Leyva, A., Contreras-Vergara, C.A., Sortillón-

428   Sortillón, A.P., Martínez-Téllez, M.A., González-Aguilar, G.A., Casas-Flores, J.S.,

429   Sañudo-Barajas, A., Kuhn, D.N., Islas-Osuna, M.A., 2019. Genome-Wide Identification

430   of Mango (Mangifera indica L.) Polygalacturonases: Expression Analysis of Family

431   Members and Total Enzyme Activity During Fruit Ripening. Front. Plant Sci. 10.

432   https://doi.org/10.3389/fpls.2019.00969

433   Dautt-Castro, M., Ochoa-Leyva, A., Contreras-Vergara, C.A., Pacheco-Sanchez, M.A.,

434   Casas-Flores, S., Sanchez-Flores, A., Kuhn, D.N., Islas-Osuna, M.A., 2015. Mango

435   (Mangifera indica L.) cv. Kent fruit mesocarp de novo transcriptome assembly identifies

436   gene families important for ripening. Front. Plant Sci. 6, 1–12.

437   https://doi.org/10.3389/fpls.2015.00062

438   El Hadi, M.A.M., Zhang, F.J., Wu, F.F., Zhou, C.H., Tao, J., 2013. Advances in fruit aroma

439   volatile research. Molecules. https://doi.org/10.3390/molecules18078200

440   Farneti, B., Gutierrez, M.S., Novak, B., Busatto, N., Ravaglia, D., Spinelli, F., Costa, G.,

441   2015. Use of the index of absorbance difference (IAD) as a tool for tailoring post-

442   harvest 1-MCP application to control apple superficial scald. Sci. Hortic. (Amsterdam).

443   190, 110–116. https://doi.org/10.1016/j.scienta.2015.04.023

444   Gapper, N.E., McQuinn, R.P., Giovannoni, J.J., 2013. Molecular and genetic regulation of

445   fruit ripening. Plant Mol. Biol. 82, 575–591. https://doi.org/10.1007/s11103-013-0050-3

446   Kamiyoshihara, Y., Iwata, M., Fukaya, T., Tatsuki, M., Mori, H., 2010. Turnover of

447   LeACS2, a wound-inducible 1-aminocyclopropane-1-carboxylic acid synthase in

448   tomato, is regulated by phosphorylation/dephosphorylation. Plant J. 64, 140–150.

449   https://doi.org/10.1111/j.1365-313X.2010.04316.x

450   Kasim, N.F.M., Mishra, P., Schouten, R.E., Woltering, E.J., Boer, M.P., 2021. Assessing

451   firmness in mango comparing broadband and miniature spectrophotometers. Infrared

452   Phys. Technol. 115, 103733. https://doi.org/10.1016/j.infrared.2021.103733

453   Lalel, H.J.D., Singh, Z., Tan, S.C., 2003. The role of ethylene in mango fruit aroma volatiles

454   biosynthesis. J. Hortic. Sci. Biotechnol. 78, 485–496.

455   https://doi.org/10.1080/14620316.2003.11511653

456   Liu, Z., Franks, R.G., 2015. Molecular basis of fruit development, Frontiers in Plant Science.

457   https://doi.org/10.3389/fpls.2015.00028

458   Luo, Y., Ge, C., Ling, Y., Mo, F., Yang, M., Jiang, L., Chen, Q., Lin, Y., Sun, B., Zhang, Y.,

459   Wang, Y., Li, M., Wang, X., Tang, H., 2020. ABA and sucrose co-regulate strawberry

460   fruit ripening and show inhibition of glycolysis. Mol. Genet. Genomics 295, 421–438.

461   https://doi.org/10.1007/s00438-019-01629-w

462   Nassur, R. de C.M.R., González-Moscoso, S., Crisosto, G.M., Lima, L.C. de O., Vilas Boas,

463   E.V. de B., Crisosto, C.H., 2015. Describing Quality and Sensory Attributes of 3 Mango

464   (*Mangifera indica* L.) Cultivars at 3 Ripeness Stages Based on Firmness. J. Food Sci.

465   80, S2055–S2063. https://doi.org/10.1111/1750-3841.12989

466   Osorio, S., Scossa, F., Fernie, A.R., 2013. Molecular regulation of fruit ripening. Front. Plant

467   Sci. 4, 1–8. https://doi.org/10.3389/fpls.2013.00198

468   Pattyn, J., Vaughan-Hirsch, J., Van de Poel, B., 2021. The regulation of ethylene

469   biosynthesis: a complex multilevel control circuitry. New Phytol.

470   https://doi.org/10.1111/nph.16873

471   Paul, V., Pandey, R., Malik, S.K., 2019. Varietal variations in rate of ripening and respiration

472   of mango (Mangifera indica L.) fruits: anatomical substantiation. Plant Physiol. Reports

473   24, 340–350. https://doi.org/10.1007/s40502-019-00466-8

474   Payasi, A., Mishra, N.N., Chaves, A.L.S., Singh, R., 2009. Biochemistry of fruit softening:

475   An overview. Physiol. Mol. Biol. Plants 15, 103–113. https://doi.org/10.1007/s12298-

476   009-0012-z

477   Schouten, R.E., Fan, S., Verdonk, J.C., Wang, Y., Kasim, N.F.M., Woltering, E.J., Tijskens,

478   L.M.M., 2018. Mango firmness modeling as affected by transport and ethylene

479   treatments. Front. Plant Sci. 871, 1647. https://doi.org/10.3389/fpls.2018.01647

480   Seymour, G.B., Poole, M., Giovannoni, J.J., Tucker, G.A., 2013. The Molecular Biology and

481   Biochemistry of Fruit Ripening, The Molecular Biology and Biochemistry of Fruit

482   Ripening. https://doi.org/10.1002/9781118593714

483   Simon, P., 2003. Q-Gene: Processing quantitative real-time RT-PCR data. Bioinformatics 19,

484   1439–1440. https://doi.org/10.1093/bioinformatics/btg157

485   Singh, Z., Singh, R.K., Sane, V.A., Nath, P., 2013. Mango - Postharvest Biology and

486   Biotechnology. CRC. Crit. Rev. Plant Sci. 32, 217–236.

487   https://doi.org/10.1080/07352689.2012.743399

488   Srivastava, S., Singh, R.K., Pathak, G., Goel, R., Asif, M.H., Sane, A.P., Sane, V.A., El, H.,

489   Garray, N.B., Xu, Z., Tang, F., Wang, A., Li, Y., Xu, Y., Lin, F., Wei, Q., Wang, J.,

490   Gong, D., Li, J., Mavi, M.F., Husin, Z., Badlishah Ahmad, R., Yacob, Y.M., Farook,

491   R.S.M., Tan, W.K., Kent, L.V., Islas-Osuna, M.A., Stephens-camacho, N. a, Contreras-

492   vergara, C.A., Rivera-dominguez, M., Sanchez-sanchez, E., Villegas-ochoa, M. a,

493   Gonzalez-aguilar, G. a, Box, P.O., Rd, H., Navojoa, K., Chin, C.F., Teoh, E.Y., Chee,

494   M.J.Y., Al-Obaidi, J.R., Rahmad, N., Lawson, T., Costa, G., Noferini, M., Fiori, G.,

495   Torrigiani, P., Dautt-Castro, M., Ochoa-Leyva, A., Contreras-vergara, C.A., Pacheco-

496   Sanchez, M.A., Casas-Flores, S., Sanchez-Flores, A., Kuhn, D.N., Islas-Osuna, M.A.,

497   López-Virgen, A.G., Ochoa-Leyva, A., Contreras-vergara, C.A., Sortillón-Sortillón,

498   A.P., Martínez-Téllez, M.A., González-Aguilar, G.A., Casas-Flores, J.S., Sañudo-

499   Barajas, A., Kuhn, D.N., Islas-Osuna, M.A., Chidley, H.G., Deshpande, A.B., Oak, P.S.,

500   Pujari, K.H., Giri, A.P., Gupta, V.S., Martin, M., He, Q., Singh, Z., Singh, R.K., Sane,

501   V.A., Nath, P., Ntsoane, M.L., Zude-Sasse, M., Mahajan, P., Sivakumar, D., Paul, V.,

502   Pandey, R., Malik, S.K., Ma, X., Zheng, B., Ma, Y., Xu, W., Wu, H., Wang, S., Shamili,

503   M., Yashoda, H.M., Prabha, T.N., Tharanathan, R.N., 2019. Comparative transcriptome

504   analysis of unripe and mid-ripe fruit of Mangifera indica (var. "Dashehari") unravels

505   ripening associated genes. Sci. Hortic. (Amsterdam). 6, 32557.

506   https://doi.org/10.1038/srep32557

507   Tucker, G., Yin, X., Zhang, A., Wang, M., Zhu, Q., Liu, X., Xie, X., Chen, K., Grierson, D.,

508   2017. Ethylene and Fruit Softening. Food Qual. Saf.

509   https://doi.org/10.1093/fqsafe/fyx024

510   Uluisik, S., Seymour, G.B., 2020. Pectate lyases: Their role in plants and importance in fruit

511   ripening. Food Chem. 309, 125559. https://doi.org/10.1016/j.foodchem.2019.125559

512   Van de Poel, B., Bulens, I., Markoula, A., Hertog, M.L.A.T.M., Dreesen, R., Wirtz, M.,

513   Vandoninck, S., Oppermann, Y., Keulemans, J., Hell, R., Waelkens, E., de Proft, M.P.,

514   Sauter, M., Nicolai, B.M., Geeraerd, A.H., 2012. Targeted systems biology profiling of

515   tomato fruit reveals coordination of the Yang cycle and a distinct regulation of ethylene

516   biosynthesis during postclimacteric ripening. Plant Physiol. 160, 1498–1514.

517   https://doi.org/10.1104/pp.112.206086

518   Van Der Straeten, D., Kanellis, A., Kalaitzis, P., Bouzayen, M., Chang, C., Mattoo, A.,

519   Zhang, J.S., 2020. Editorial: Ethylene Biology and Beyond: Novel Insights in the

520   Ethylene Pathway and Its Interactions, Frontiers in Plant Science.

521   https://doi.org/10.3389/fpls.2020.00248

522   Watkins, C.B., 2006. The use of 1-methylcyclopropene (1-MCP) on fruits and vegetables.

523   Biotechnol. Adv. https://doi.org/10.1016/j.biotechadv.2006.01.005

524 Wehrens, R., 2011. Chemometrics with R, Chemometrics with R. Springer Berlin

525   Heidelberg. https://doi.org/10.1007/978-3-642-17841-2

526 Zaharah, S.S., Singh, Z., Symons, G.M., Reid, J.B., 2012. Role of Brassinosteroids, Ethylene,

527   Abscisic Acid, and Indole-3-Acetic Acid in Mango Fruit Ripening. J. Plant Growth

528   Regul. 31, 363–372. https://doi.org/10.1007/s00344-011-9245-5

529 Zhang, D.P., 2014. Abscisic acid: Metabolism, transport and signaling, Abscisic Acid:

530   Metabolism, Transport and Signaling. https://doi.org/10.1007/978-94-017-9424-4

531 Zhang, J., Ma, Y., Dong, C., Terry, L.A., Watkins, C.B., Yu, Z., Cheng, Z.M. (Max), 2020.

532   Meta-analysis of the effects of 1-methylcyclopropene (1-MCP) treatment on climacteric

533   fruit ripening. Hortic. Res. 7, 208. https://doi.org/10.1038/s41438-020-00405-x

534 Ziosi, V., Noferini, M., Fiori, G., Tadiello, A., Trainotti, L., Casadoro, G., Costa, G., 2008. A

535   new index based on vis spectroscopy to characterize the progression of ripening in peach

536   fruit. Postharvest Biol. Technol. 49, 319–329.

537   https://doi.org/10.1016/j.postharvbio.2008.01.017

538

539 FIGURE CAPTIONS

540 **Figure 1.** Characterization of ripening associated parameters over the five timepoints included

541 in the experimental design. a) I_{AD} change during the shelf life; b) texture parameter reported as

542 the F(1) measurement (expressed in Newton); c) soluble solid content (SSC; %); d) ethylene

543 quantification. Error bars represent the standard deviation. Different letters above each point

544 indicate significative differences between each sampling time.

545 **Figure 2.** Example of texture profile for each stage included in the time course. The mechanical

546 displacement was defined by the y-axes, representing the force values (in Newton), and the x-

547 axes, indicating the probe's travel (distance, in mm). In green the texture profile at 1 d stage

548 while in yellow, orange, dark orange and red the different profiles measured at 5d, 9d, 12d and

549   15d, respectively. On the right panel the profiles from 5d to 15d are magnified with a different

550   scale. The gray dotted line marks the position of the first mechanical peak (F1).

551   **Figure 3.** Expression analysis of six genes belonging to the ethylene pathway and selected to

552   characterize the fruit ripening of Keitt mango fruit. The expression was reported for each

553   sample of the time course, and it was represented as mean normalized expression. Error bars

554   represent the standard deviation. Different letters above each bar indicate significative

555   differences.

556   **Figure 4.** Expression profile of seven genes, involved in the cell wall metabolism (a, b, c, d, e)

557   and carotenoids accumulation (f, g) of Keitt mango fruit. As for Fig.2, gene expression was

558   illustrated as mean normalized expression. Error bars represent the standard deviation.

559   Different letters above each bar indicate significative differences.

560   **Figure 5.** 2D-PCA plot illustrating the whole variability among the different timepoints based

561   on their transcriptomic profiles, I_{AD}, texture modification and soluble solid content (SSC). a)

562   score plot showing the distribution of the five different stages on the PCA space. b) loading

563   plot of each variable employed in this analysis.

564   **Suppl. Table 1.** List of primers used for the transcriptomic investigation of the gene set

565   employed in this survey. In the table the ID for each gene, the forward and reverse primer

566   sequences and the gene acronym are reported, together with the gene function and the related

567   pathway. On the right, for each primer pair, the DOI number referred to the paper where the

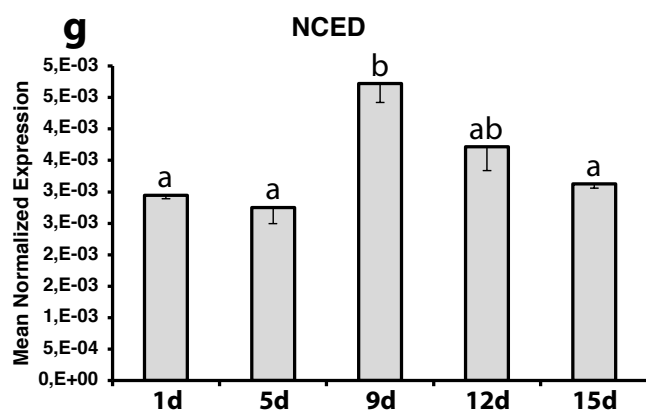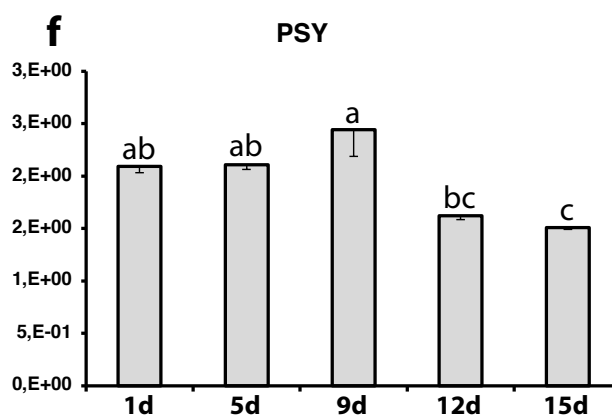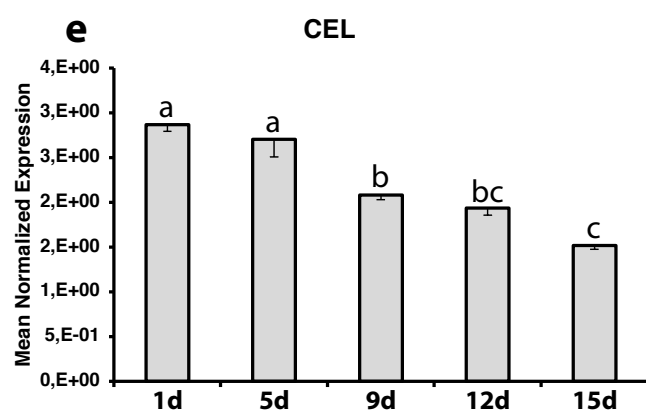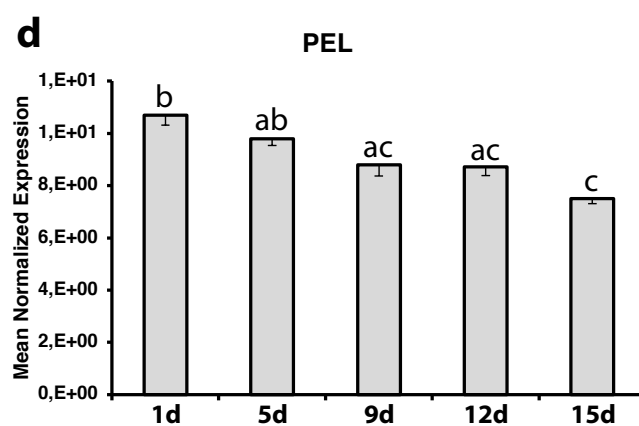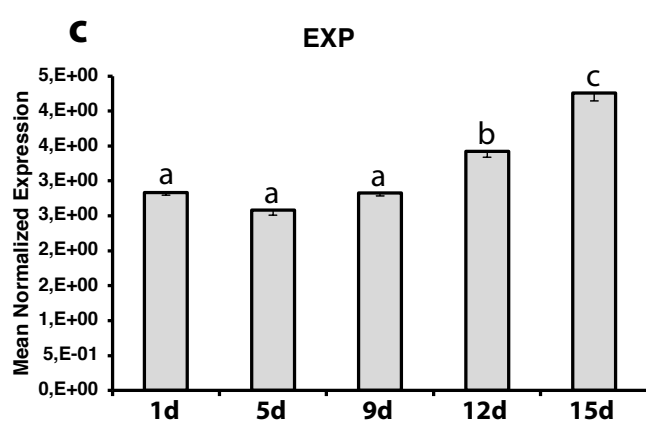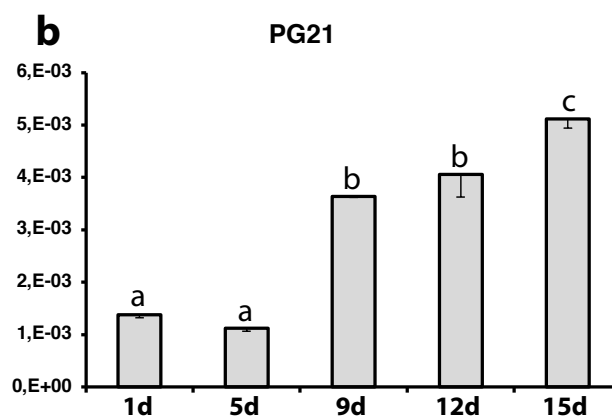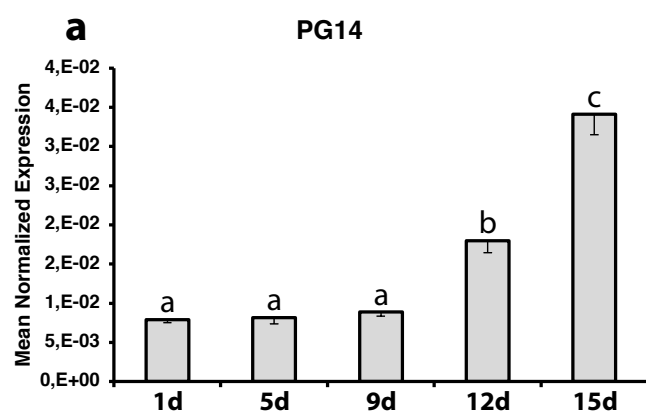568   primers were originally published was reported.

569   **Suppl. Figure 1.** a) heatmaps representing the kinetics of I_{AD} values over the four time points

570   comprised in the experimental design. White blocks correspond to fruit that rotted before the

571   end of the survey. Each value was calculated as the average of three independent

572   measurements. b) pictures of the fruit taken at each time point. Missing images correspond to

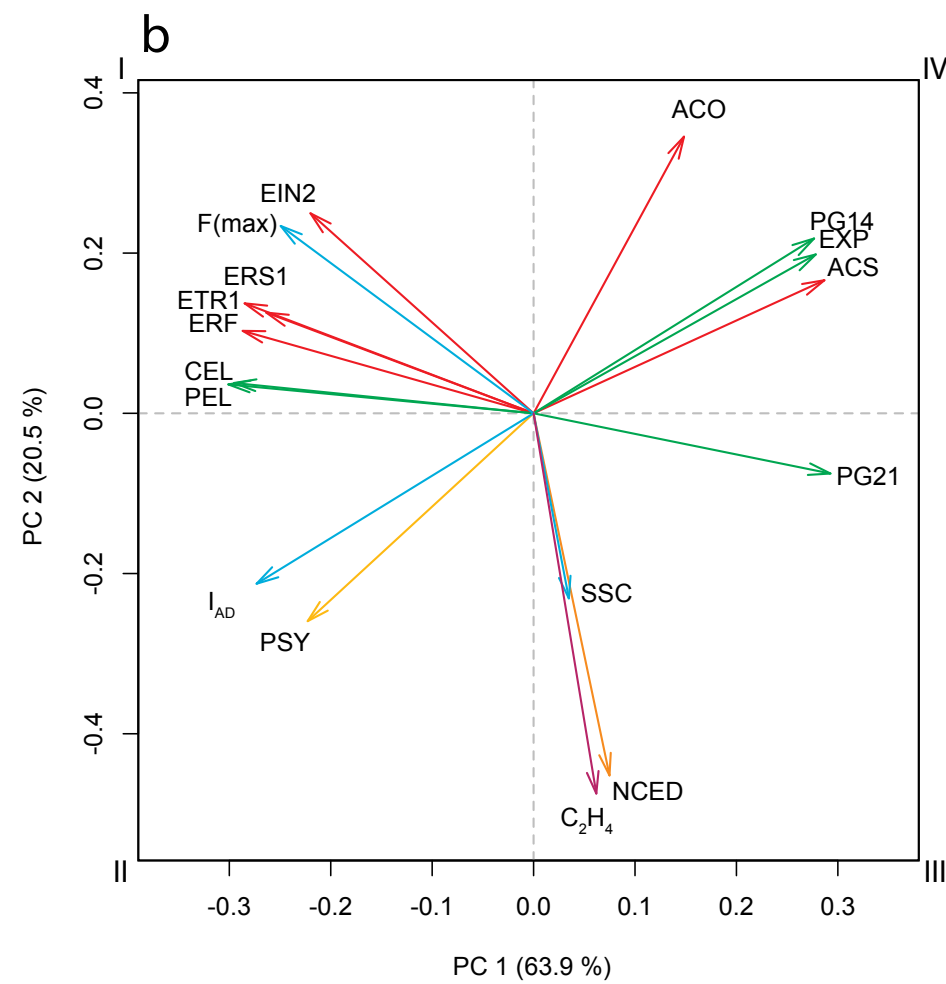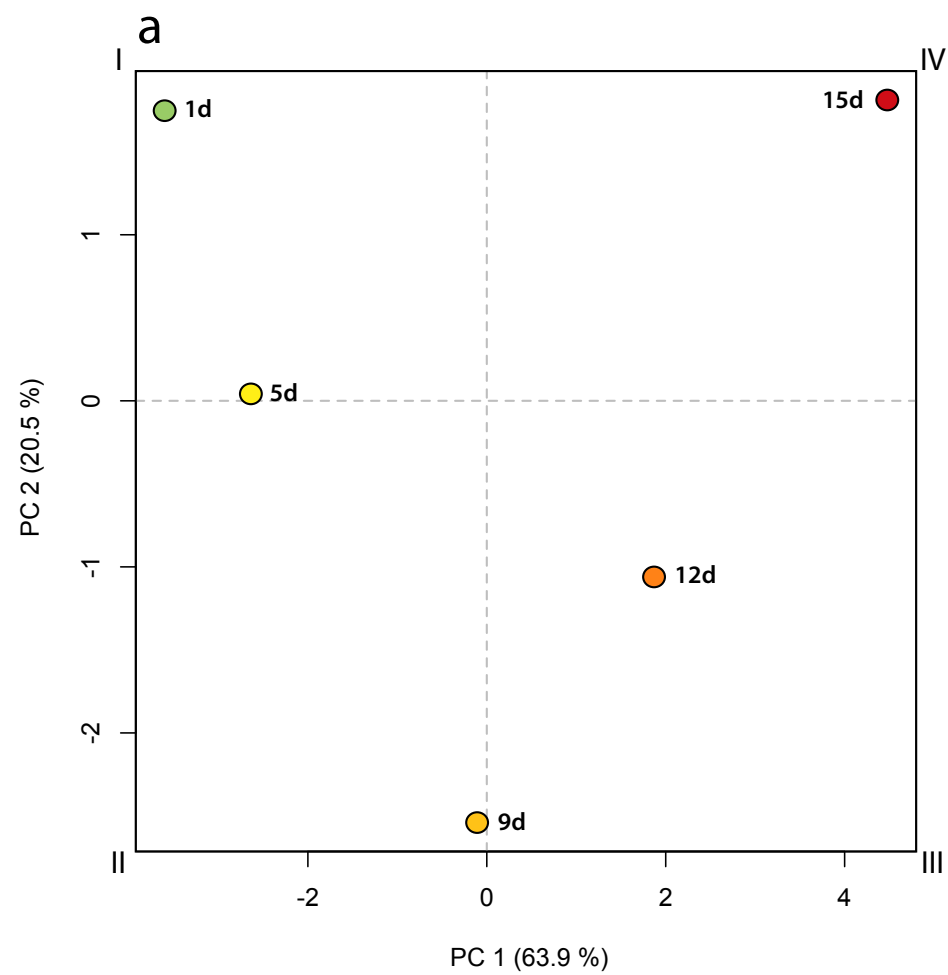573   compromised fruit, due to senescence decay.

574 **Suppl. Figure 2.** Model summarizing the evolution of I_{AD} values monitored in four different

575 trays containing nine fruit each, over the five time points comprised in the experimental design.

576 The black line represents the regression curve calculated approximating the I_{AD} changes plotted

577 for each single fruit (dotted lines) visualized in the Suppl. Fig. 1a. Black dots represent the I_{AD}

578 values measured on the fruit used for the destructive analysis (as indicated in Fig. 1a). The

579 model was calculated using R (tidyverse and ggplot2 libraries).

Fig_1

Click here to access/download;Figure;Fig_1.pdf ±

a **DA-meter**

b **Firmness**

c **SSC**

d **Ethylene**

Fig_2

Click here to access/download;Figure;Fig_2.pdf ⬧

Texture

Fig_3

Click here to access/download;Figure;Fig_3.pdf ⬇

Fig_4   Click here to access/download;Figure;Fig_4.pdf ⬇

Fig_5 ⬇
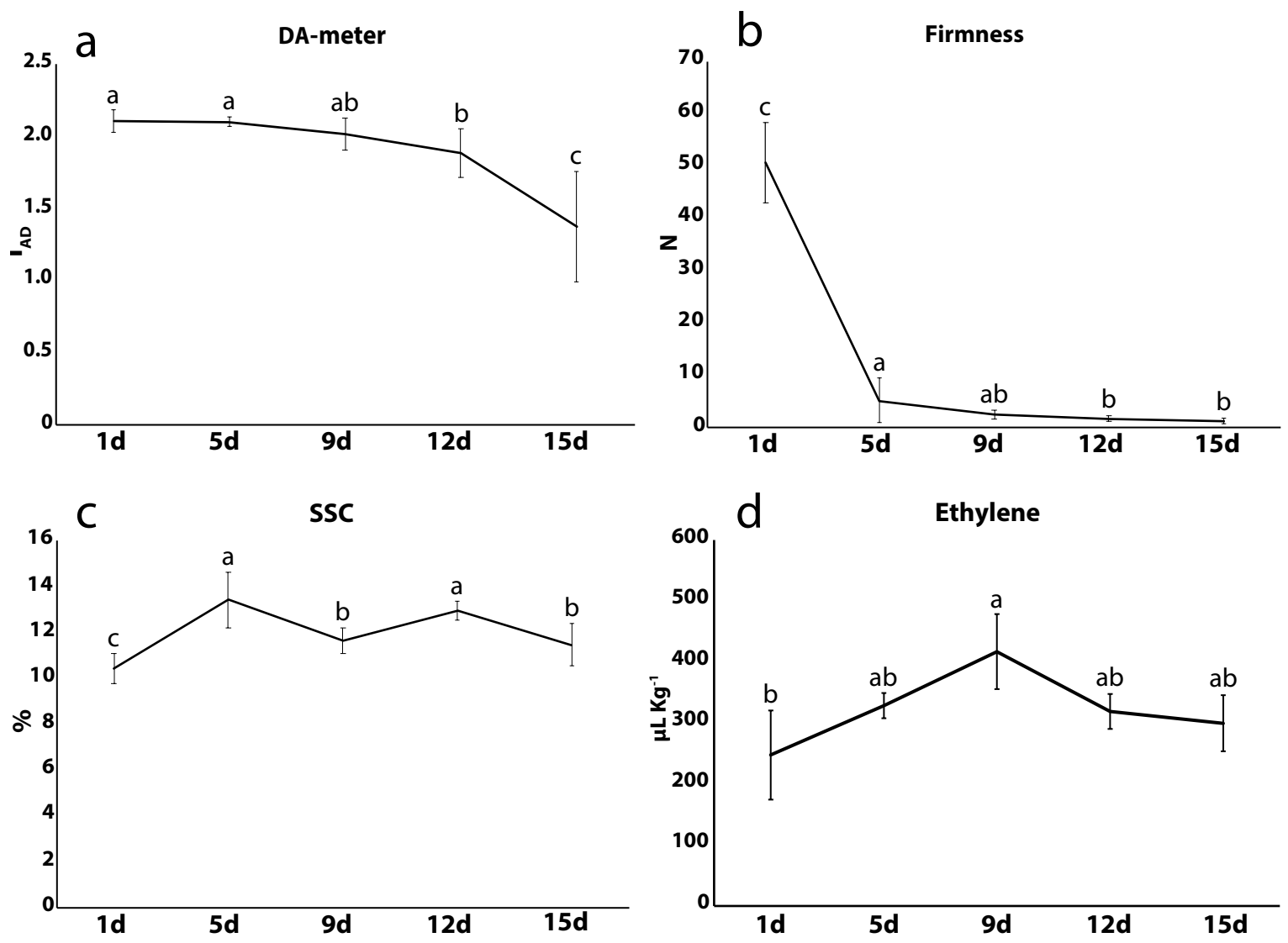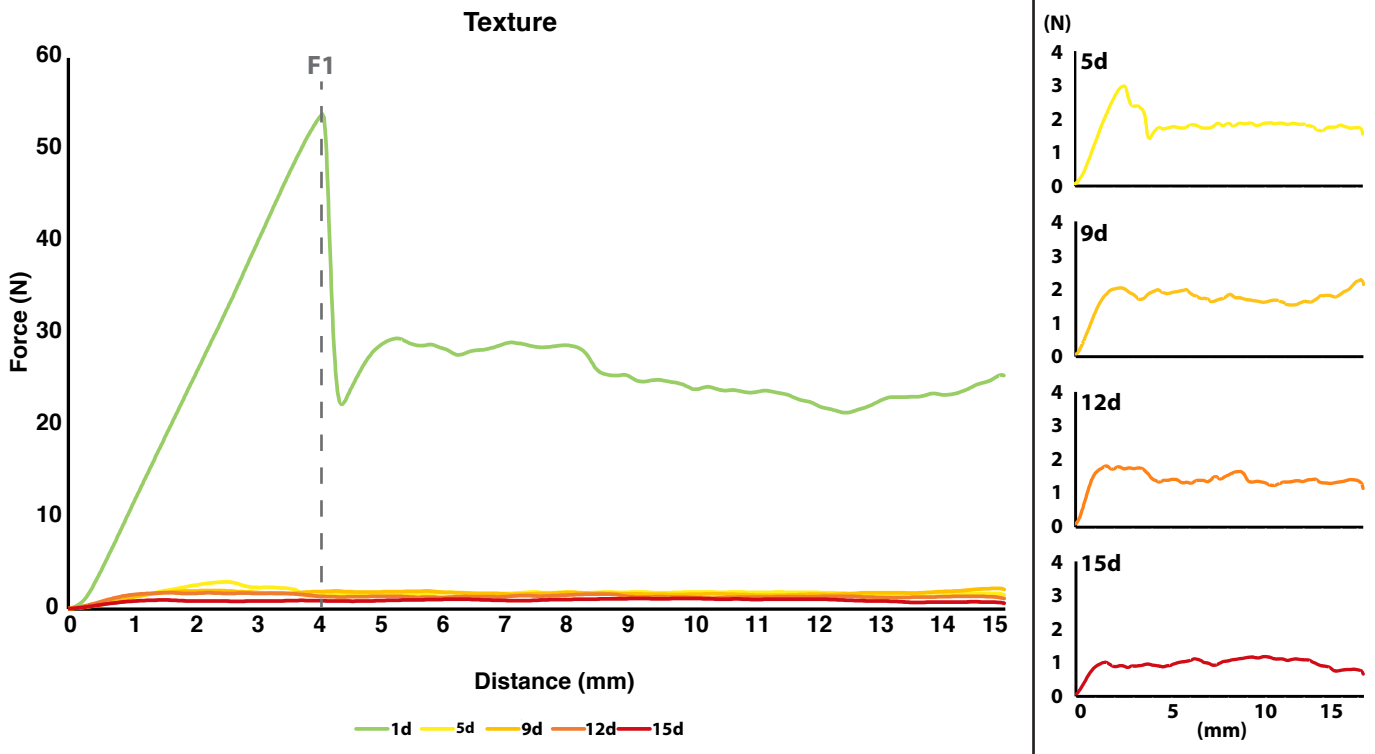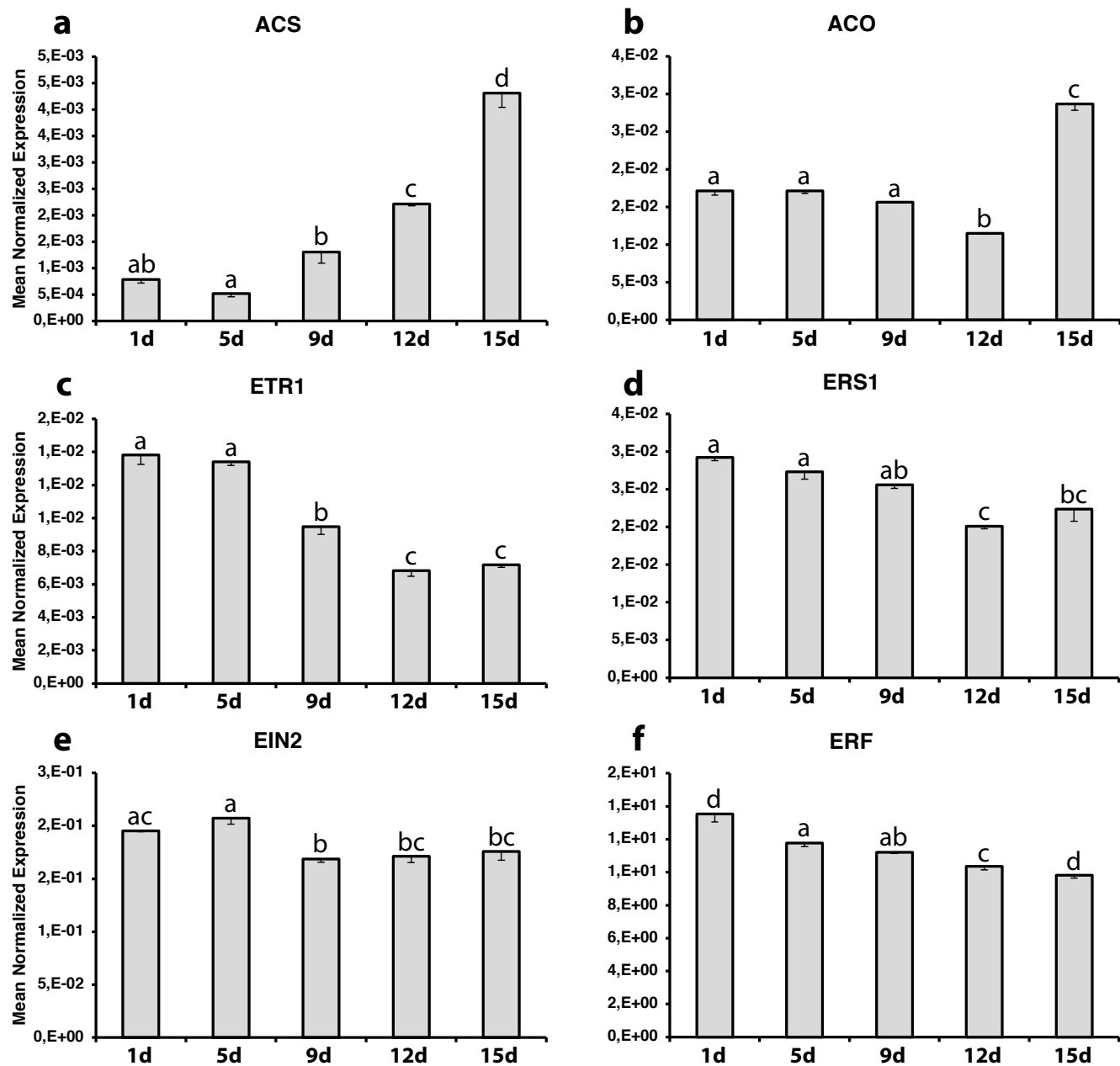
Declaration of interests

☒ The authors declare that they have no known competing financial interests or personal relationships that could have appeared to influence the work reported in this paper.

☐The authors declare the following financial interests/personal relationships which may be considered as potential competing interests:

Author contributions

Nicola Busatto: investigation, original draft preparation, conceptualization; **Lorenzo Vittani**: investigation; **Brian Farneti**: editing, investigation; **Iuliia Khomenko**: investigation; **Matteo Caffini**: editing; **Marco Boschetti**: funding acquisition, editing; **Fabrizio Costa**: writing, editing, supervision.

Click here to access/download
Supplementary Material
Suppl_Tab_1.xlsx
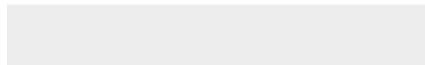
Suppl_Fig1

Click here to access/download
Supplementary Material
Suppl_Fig_1.pdf

Suppl_Fig2

Click here to access/download
Supplementary Material
Suppl_Fig_2.pdf